Inorganic Chemistry

Article

pubs.acs.org/IC

Chelating and Linking $S_4O_{13}^{2-}$ Anions: Synthesis and Characterization of the *Bis*-(tetrasulfato) Palladates $M_2[Pd(S_4O_{13})_2]$ (M = NH_4, Rb, NO) and the Sodium Palladium Tetrasulfate $Na_2Pd(S_4O_{13})_2$

Jörn Bruns, Mareike Hänsch, and Mathias S. Wickleder*

Institute of Chemistry, Carl von Ossietzky University of Oldenburg, Carl-von-Ossietzky-Str. 9-11, 26129 Oldenburg, Germany

Supporting Information

ABSTRACT: The reaction of SO_3 with either the palladium chlorides M_2PdCl_6 (M = Rb, NH_4) or the nitrato-palladate $(NO)_2[Pd(NO_3)_4]$ at elevated temperature led to yellow single crystals of the complex palladates $M_2[Pd(S_4O_{13})_2]$ (M = NH_4: triclinic, $P\bar{1}$, a = 7.3882(3) Å, b = 8.5223(3) Å, c = 9.2712(4) Å, α = 71.945(2)°, β = 88.910(2)°, γ = 72.603(2)°, V = 527.88(4) Å^3; M = NO: triclinic, $P\bar{1}$, a = 7.2881(3) Å, b = 8.9125(2) Å, c = 8.9220(4) Å, α = 75.546(2)°, β = 89.151(2)°, γ = 69.516(2)°, V = 524.02(4) Å^3; M = Rb: triclinic, $P\bar{1}$, a = 7.4468(4) Å, b = 8.5066(4) Å, c = 9.2477(4) Å, α = 72.321(2)°, β = 88.512(2)°, γ = 72.128(2)°, V = 529.75(4) Å^3). In the isotypic compounds, the Pd atom is in square planar oxygen coordination, achieved by two bidentate-chelating tetrasulfate anions. The reaction of Na_2PdCl_6 with neat SO_3 afforded yellow crystals of $Na_2Pd(S_4O_{13})_2$ (monoclinic, $P2_1/c$, a = 6.9953(4) Å, b = 15.9420(9) Å, c = 9.2299(5) Å, β = 100.235(2)°, V = 1012.45(1) Å^3). The structure exhibits no palladate complexes but an anionic two-dimensional network, according to $^2_\infty[Pd(S_4O_{13})_{4/2}]^{2-}$. The latter shows the tetrasulfate anions acting as bidentate-bridging ligands. The tetrasulfato-palladates were studied in more detail by means of thermal analyses and infrared (IR) spectroscopy. The observed IR bands were assigned according to quantum chemical calculations performed on the anion $[Pd(S_4O_{13})_2]^{2-}$.

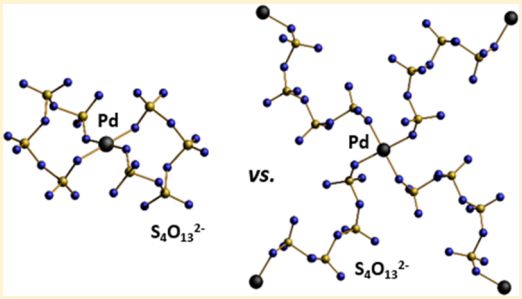

1. INTRODUCTION

Sulfuric acid is one of the most fundamental chemical substances, and the technical process of its production is a highly important procedure in industrial chemistry. This so-called *contact process* involves disulfuric acid ($H_2S_2O_7$) as a crucial intermediary product that forms when gaseous SO_3 is passed into concentrated sulfuric acid. Formally, $H_2S_2O_7$ is the condensation product of two molecules of H_2SO_4. In principle, further condensation might occur, leading to polysulfuric acids with increasing chain lengths of the general formula H-$(SO_3)_n$OH. Although these type of compounds are mentioned in numerous chemistry textbooks, to date, nothing is known about their structures and properties. The only exception is $H_2S_2O_7$, which was structurally characterized in 1991.[1] The situation is only slightly better for the respective salts of polysulfuric acids. Although the first hydrogen disulfate was already presented in 1954 in the form of $(NO_2)(HS_2O_7)$,[2] and the first disulfate, $K_2(S_2O_7)$, was published as early as 1960,[3] most of the known disulfates have been presented quite late, with recent contributions from our group as well.[2−19] Concerning higher polysulfates, there are significantly fewer examples. Until recently, there was only one structure determination for a trisulfate, namely, the nitrylium trisulfate, $(NO_2)_2(S_3O_{10})$, originally reported by Eriks and MacGillavry in 1954,[20] but later corrected by Cruickshank in 1964.[21] Recently, we contributed two further examples: the lead trisulfate $Pb(S_3O_{10})$,[22] and the heteroleptic palladate $Ba_2[Pd(HS_2O_7)_2(S_3O_{10})_2]$.[23] Surprisingly, there is also an early report on the pentasulfate $K_2(S_5O_{16})$ that has been structurally characterized by film techniques in 1969.[24] Only a few years ago, we were able to provide the first tetrasulfate anion as a missing link in the row.[25] The anion could be isolated in the form of the salt $(NO_2)_2(S_4O_{13})$, obtained from the reaction between N_2O_5 and SO_3. Detailed inspection of the tetrasulfate anion in this compound revealed that the bond length differences within the S−O−S bridges of the anion's backbone are significantly larger for the terminal tetraheda of the tetrasulfate anion. High-level theoretical investigations confirmed these findings and predicted that the asymmetry in the S−O−S bridges will even increase for long-chain polysulfates.[25] Thus, it is not very likely that long-chain polysulfate anions can be easily prepared. In order to stabilize polysulfate anions, we attempted the formations of complexes using this type of anion as a ligand. These attempts led to the first complex tetrasulfate, $K_2[Pd(S_4O_{13})_2]$, prepared via the reaction of K_2PdCl_4 with SO_3 at 120 °C.[26] Indeed, the chelating coordination of the Pd atom by tetrasulfate groups leads to a stabilization of the anions, at least with respect to the increasing symmetry in the S−O−S bridges, compared to the tetrasulfate anion in $(NO_2)_2(S_4O_{13})$.[25]

Received: January 26, 2015
Published: May 26, 2015

DOI: 10.1021/acs.inorgchem.5b00195
Inorg. Chem. 2015, 54, 5681−5690

Here, we report further representatives of the $[Pd(S_4O_{13})_2]^{2-}$ anion. The substitution of potassium by ammonium or nitrosylium cations and even by the larger rubidium cation leads to the compounds $M_2[Pd(S_4O_{13})_2]$ (where M = NH_4, Rb, NO), which are isotypic with their potassium (K) congener. Interestingly, if the smaller alkaline-metal ion Na^+ is used as a countercation, the coordination mode of the tetrasulfate anion changes. It is no longer a bidentate-chelating ligand for one Pd^{2+} cation but a bidentate-bridging one between two metal cations. Thus, the new sodium compound $Na_2Pd(S_4O_{13})_2$ is the first example of a tetrasulfate anion embedded in an anionic network.

2. EXPERIMENTAL SECTION

2.1. Synthesis. For the preparation of $M_2[Pd(S_4O_{13})_2]$ (M = NH_4, Rb) and $Na_2Pd(S_4O_{13})_2$, 0.055 g of M_2PdCl_6 (M = NH_4, Rb, Na), which was obtained according to ref 27, were used as starting material. The nitrosylium compound $(NO)_2[Pd(S_4O_{13})_2]$ was prepared starting from 0.056 g of $(NO)_2[Pd(NO_3)_4]$ that was obtained according to ref 28. In any case, the starting materials were loaded into thick-walled glass ampules (l = 250 mm, ⌀ = 20 mm, thickness of the tube wall = 2 mm). For the generation of SO_3, a 500 mL three-necked flask was filled with 30 g of P_4O_{10} and connected to a dropping funnel filled with 30 mL of oleum (65% SO_3). By heating to 120 °C, SO_3 was driven off and condensed into the ampules by cooling the latter with liquid nitrogen. The ampules were torch-sealed, placed into a tube furnace, and heated to 120 °C. The temperature was maintained for 2 days and finally reduced to 25 °C within 150 h. A large number of orange−yellow crystals was obtained, and the yield was quantitative, with respect to the initial palladium compounds, except for the sodium compound. For the latter, the amount of yellow crystals was quite low. A yellowish byproduct was obtained, which, to date, could not be identified.

Caution! *Oleum and SO_3 are strong oxidizers, which require careful handling. During and even after the reaction, the ampule might be under remarkable pressure. The ampule must be cooled with liquid nitrogen prior to opening. The obtained crystalline material of each tetrasulfate compound is extremely moisture-sensitive. Therefore, the crystals must be handled under strictly inert conditions.*

2.2. X-ray Crystallography. Several single crystals of each compound were transferred into inert oil. A suitable specimen was selected unter a polarization microscope. The chosen crystal was mounted onto a glass needle (⌀ = 0.1 mm) and immediately placed into a stream of cold N_2 (−120 °C) inside the diffractometer (κ-APEX II, Bruker, Karlsruhe, Germany). After unit cell determination, the reflection intensities were collected.

$M_2[Pd(S_4O_{13})_2]$ (M = NH_4, Rb). Assuming the space group $P\bar{1}$, the structure solution was successful using Direct Methods, as provided by SHELXS-97.[29] The solution provided the positions of the Pd and S atoms, as well as of some O atoms and the Rb atom. The remaining O atoms and the N atom, in the case of $(NH_4)_2[Pd(S_4O_{13})_2]$, could be located in the Fourier maps during the refinement with SHELXL-97.[29] A numerical absorption correction was applied to the data using the programs X-RED 1.22 and XSHAPE 1.06,[30,31] and all non-hydrogen atoms were refined anisotropically. For $(NH_4)_2[Pd(S_4O_{13})_2]$, the H atoms were refined without restraints. Finally, the structure model refined to R_1 = 0.0196 and wR_2 = 0.0474 (all data) for $(NH_4)_2[Pd(S_4O_{13})_2]$, and to R_1 = 0.0155 and wR_2 = 0.0393 (all data) for $Rb_2[Pd(S_4O_{13})_2]$.

$(NO)_2[Pd(S_4O_{13})_2]$. Assuming the space group $P\bar{1}$ for $(NO)_2[Pd(S_4O_{13})_2]$, the application of Direct Methods, as provided by SHELXS-2013,[29] revealed the position of the Pd and S atoms, as well as of some O atoms. The remaining O atoms and the N atom could be located in Fourier maps during the refinement with SHELXL-2013.[29] A numerical absorption correction was applied to the data using the program SADABS-2012/1,[32] and all atoms were refined anisotropically. Finally, the structure model refined to R_1 = 0.0156 and wR_2 = 0.0428 for all data.

$Na_2Pd(S_4O_{13})_2$. Assuming the space group $P2_1/n$ for $Na_2Pd(S_4O_{13})_2$, the application of Direct Methods as provided by SHELXS-97[29] revealed the position of the Pd and S atoms, as well as some of the O atoms and natrium. The remaining O atoms could be located in Fourier maps during the refinement with SHELXL-97.[29] A numerical absorption correction was applied to the data using the programs X-RED 1.22 and XSHAPE 1.06,[30,31] and all atoms were refined anisotropically. Finally, the structure model was refined to R_1 = 0.0137 and wR_2 = 0.0376 for all data.

2.3. Thermal Analysis. The investigations of the thermal behavior of the complex tetrasulfato-palladates were performed using a thermoanalyzer (Model TGA/DSC1, Mettler−Toledo GmbH, Schwerzenbach, Switzerland). For that purpose, ∼5−10 mg of each compound were placed in a corundum crucible and heated in a flow of dry nitrogen at a rate of 10 K/min up to 1050 °C. The collected data were processed using the software of the analyzers (Model STARe V9.3, Mettler−Toledo).[33]

2.4. Powder X-ray Diffraction. The obtained residual products of the thermoanalytical measurements were prepared on a flat sample holder. The diffraction patterns were measured with a diffractometer (Model STADIP, Stoe), using Cu Kα radiation (λ = 1.5406 Å). The diffraction data were processed with the WinXPow 2007 program package (Stoe, V. 2.20).[34]

2.5. IR Spectroscopy. Because of their sensitivity, the samples of the respective tetrasulfato-palladates $M_2[Pd(S_4O_{13})_2]$ (M = NH_4, Rb, NO) were mounted to the sample holder of a FTIR spectrometer (Platinum ATR, Tensor 27, Bruker) in a glovebox and measured immediately. The IR data were processed using the program OPUS 6.5.[35] The spectra were measured in the energy region of 550−3500 cm^{-1}.

3. RESULTS AND DISCUSSION

3.1. Crystal Structures of $M_2[Pd(S_4O_{13})_2]$ (M = NH_4, NO, Rb). All palladates, obtained as yellow plate-shaped crystals (Figure 1; also see Figure S1 in the Supporting Information),

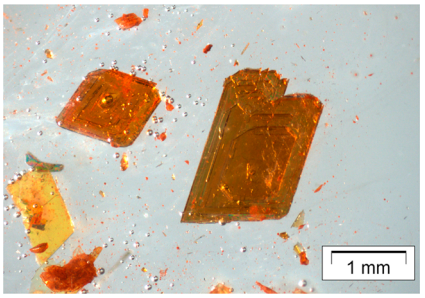

Figure 1. Crystals of $(NH_4)_2[Pd(S_4O_{13})_2]$, viewed using a polarized microscope. The intensity of the yellow color of the crystals depends on the thickness of the plate-shaped crystals.

are isotypic with the previously reported palladate $K_2[Pd(S_4O_{13})_2]$ and crystallize with triclinic symmetry.[26] The asymmetric unit of each *bis*-(tetrasulfato)-palladate contains one Pd atom on the Wyckoff site *1h* bearing inversion symmetry, and one $S_4O_{13}^{2-}$ anion, as well as one countercation (NH_4^+, NO^+, or Rb^+) on general sites (Wyckoff position *2i*). Consequently, the two tetrasulfate anions that are bonded in a bidentate-chelating mode to the Pd^{2+} ions are symmetry equivalent. The coordination of the tetrasulfate anions leads to the formation of the anionic complex $[Pd(S_4O_{13})_2]^{2-}$ (see Figure 2). In the complex, the Pd atom is in square planar coordination by O atoms with bond lengths Pd−O of ∼2.01 Å. The bond angles O−Pd−O deviate only slightly from 90°, proving the almost-perfect shape of the $[PdO_4]$ moeitey. (For a

DOI: 10.1021/acs.inorgchem.5b00195
Inorg. Chem. 2015, 54, 5681−5690

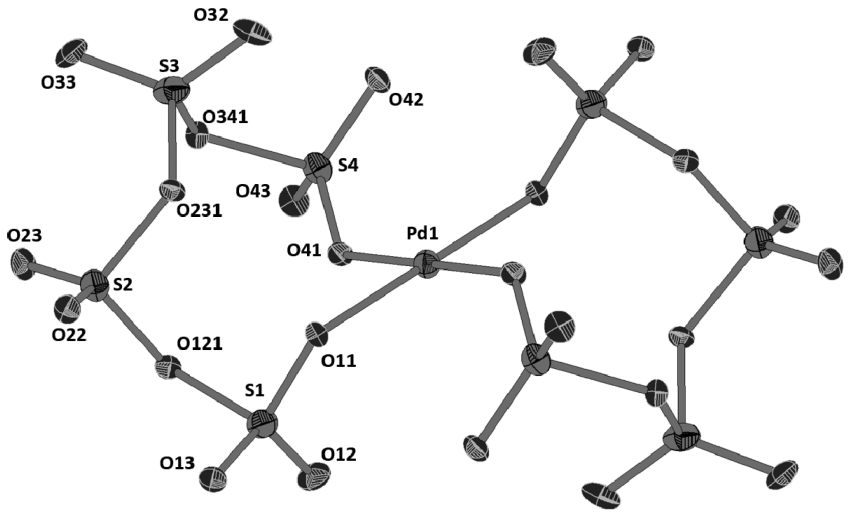

Figure 2. Structure and atom labeling of the $[Pd(S_4O_{13})_2]^{2-}$ anion in $(NH_4)_2[Pd(S_4O_{13})_2]$. The thermal ellipsoids are drawn at a 75% probability level. Both tetrasulfate groups are related by inversion symmetry at the Pd site. The compounds $M_2[Pd(S_4O_{13})_2]$ (M = Rb, NO) are isotypic. Bond lengths Pd−O: for $(NH_4)_2[Pd(S_4O_{13})_2]$, Pd1−O11 = 2.0036(7) Å, Pd1−O41 = 2.0177(7) Å; for $(NO)_2[Pd(S_4O_{13})_2]$, Pd1−O11 = 2.0050(6), 2.0137(5) Å; for $Rb_2[Pd(S_4O_{13})_2]$, Pd1−O11 = 2.0073(7), 2.0156(7) Å. For detailed bond lengths of the polysulfate anions, see Table 1. The Supporting Information gives a list of all significant bond lengths and angles of each compound.

Table 1. Bond Lengths S−O for $M_2[Pd(S_4O_{13})_2]$ (M = NH_4, NO, Rb), $Na_2Pd(S_4O_{13})_2$, and $(NO_2)_2[S_4O_{13}]$[a]

	$(NH_4)_2[Pd(S_4O_{13})_2]$		$(NO)_2[Pd(S_4O_{13})_2]$		$Rb_2[Pd(S_4O_{13})_2]$		$Na_2Pd(S_4O_{13})_2$		$(NO_2)_2[S_4O_{13}]$[25]	
	S−O (Å)	Δ	S−O (Å)	Δ	S−O (Å)	Δ	S−O (Å)	Δ	S−O (Å)	Δ
S1−O11	1.4798(7)		1.4804(6)		1.4791(7)		1.4695(5)		1.4206(10)	
S1−O12	1.4165(8)		1.4179(6)		1.4168(8)		1.4210(6)		1.4237(9)	
S1−O13	1.4220(8)		1.4201(6)		1.4225(7)		1.4190(6)		1.4246(10)	
S1−O121	*1.7036(7)*	Δ = *0.142(1)*	*1.7058(6)*	Δ = *0.142(1)*	*1.7058(7)*	Δ = *0.145(1)*	*1.7015(5)*	Δ = *0.140(1)*	*1.7644(8)*	Δ = *0.235(2)*
S2−O121	*1.5620(7)*		*1.5641(6)*		*1.5610(7)*		*1.5613(5)*		*1.5290(8)*	
S2−O22	1.4113(8)		1.4117(6)		1.4121(7)		1.4147(6)		1.4156(9)	
S2−O23	1.4091(8)		1.4089(7)		1.4096(7)		1.4131(6)		1.4120(9)	
S2−O231	*1.6247(7)*	Δ = *0.008(1)*	*1.6289(6)*	Δ = *0.020(1)*	*1.6249(7)*	Δ = *0.009(1)*	*1.6039(5)*	Δ = *0.036(1)*	*1.6389(8)*	Δ = *0.032(2)*
S3−O231	*1.6164(7)*		*1.6089(6)*		*1.6159(7)*		*1.6397(5)*		*1.6064(8)*	
S3−O32	1.4072(9)		1.4094(7)		1.4089(8)		1.4104(6)		1.4107(9)	
S3−O33	1.4134(8)		1.4137(7)		1.4148(8)		1.4094(5)		1.4230(9)	
S3−O341	*1.5600(7)*	Δ = *0.159(1)*	*1.5667(6)*	Δ = *0.144(1)*	*1.5551(7)*	Δ = *0.174(1)*	*1.5487(5)*	Δ = *0.144(1)*	*1.5344(8)*	Δ = *0.236(2)*
S4−O341	*1.7186(7)*		*1.7109(6)*		*1.7292(7)*		*1.6962(5)*		*1.7707(9)*	
S4−O41	1.4737(7)		1.4714(6)		1.4763(7)		1.4726(5)		1.4323(9)	
S4−O42	1.4216(8)		1.4230(6)		1.4190(7)		1.4171(5)		1.4392(9)	
S4−O43	1.4199(8)		1.4206(6)		1.4178(7)		1.4203(5)		1.4174(9)	

[a]Bridging S−O bonds are shown in italic font. The Δ-values (in Å) give the S−O bond length differences within a S−O−S bridge.

detailed list of bond distances and angles, see Figure 2 and Tables S3−S8 in the Supporting Information.)

Within the $S_4O_{13}^{2-}$ anions, the distances S−O for the terminal oxygen atoms (O12, O13, O22, O23, O32, O33, O42, and O43) are found quite uniformly at ∼1.41 Å (see Table 1). The O atoms coordinated to the Pd^{2+} ion show longer S−O distances with values at ∼1.47 Å (O11 and O41). The S−O bond lengths within the central S2−O231−S3 bridges are in the narrow range between 1.61 and 1.63 Å. Thus, the differences between the bonds within the S−O−S bridges are small, 0.008(1) Å for M = NH_4, 0.020(1) Å for M = NO, 0.009(1) Å for M = Rb (Table 1). These values are slightly smaller than the 0.032(1) Å observed for the "free" tetrasulfate anion in $(NO_2)_2(S_4O_{13})$. The outer S−O−S bridges in the $[Pd(S_4O_{13})_2]^{2-}$ complexes exhibit larger bond length differences in all of the investigated compounds. These differences range from 0.142(1) to 0.174(1) Å (Table 1). However, these values are significantly smaller than observed for the tetrasulfate anions in $(NO_2)_2(S_4O_{13})$, which show bond length differences as large as 0.24 Å (see Table 1).

Charge compensation for the $[Pd(S_4O_{13})_2]^{2-}$ anions is achieved by the counter cations NH_4^+, NO^+, and Rb^+,

DOI: 10.1021/acs.inorgchem.5b00195
Inorg. Chem. 2015, 54, 5681−5690

respectively. If distances up to 3.40 Å are taken into account, the cations reveal a coordination number of 10, which is consistent with electrostatic calculations (see Table 2).[36] The Rb^+ and NH_4^+ ions have almost the same size, so the distances to the O atoms are very similar. Because of the nonspherical shape of the NO^+ cation, the situation is slightly different for that molecule. The distance N−O within the cation is 1.041(1) Å, which is consistent with the findings of other nitrosylium compounds (e.g., $(NO)_2[Pd(NO_3)_4]$).[28] For a reliable comparison with the distances M−O observed for M = Rb^+ and NH_4^+, we calculated the distances between the midpoint of the N−O bond and the surrounding O atoms. It turned out that the distances are similar, but, nevertheless, the special shape of the cation is reflected by the observed distance alterations (one distance is even enlarged up to 3.63 Å). Even if the NO^+ ion is not spherical, its volume requirement seems to be very similar to those of Rb^+ and NH_4^+, as can be seen from the similar volumes of the unit cells (see Table 3). However, the rod shape of the cation influences the unit-cell parameters. Thus, the crystallographic *b*-axis of $(NO)_2[Pd(S_4O_{13})_2]$ is elongated by ∼0.40 Å, compared to its Rb^+ and NH_4^+ congeners, because of the orientation of the cation along the [010] direction. In turn, the other two axes of the unit cell are

Table 2. Observed M−O Bond Lengths in the Structure of $M_2[Pd(S_4O_{13})_2]$ (M = NH_4, NO, Rb)

	Bond Length (Å)		
M^+−O bond	M = NH_4	M = NO	M = Rb
M^+−O12	2.890(1)	2.607(8)	2.8679(7)
M^+−O13	3.036(1)	3.067(8)	3.0549(7)
M^+−O13	3.117(1)	3.321(8)	3.0951(7)
M^+−O22	3.051(1)	2.850(8)	3.0343(7)
M^+−O23	2.959(1)	3.256(8)	2.9951(7)
M^+−O32	3.090(1)	3.193(8)	3.0673(9)
M^+−O33	3.016(1)	2.847(8)	3.0540(8)
M^+−O33	3.289(1)	3.631(8)	3.273(1)
M^+−O42	2.983(1)	2.670(8)	3.0213(7)
M^+−O43	2.985(1)	2.674(8)	2.9663(7)

Table 3. Crystallographic Data of $M_2[Pd(S_4O_{13})_2]$ (M = NH_4, NO, Rb) and $Na_2Pd(S_4O_{13})_2$

property	$(NH_4)_2[Pd(S_4O_{13})_2]$	$(NO)_2[Pd(S_4O_{13})_2]$	$Rb_2[Pd(S_4O_{13})_2]$	$Na_2Pd(S_4O_{13})_2$
molar mass	814.96 g/mol	838.90 g/mol	949.82 g/mol	824.86 g/mol
temperature	120(2) K	120(2) K	120(2) K	120(2) K
wavelength	0.71073 Å	0.71073 Å	0.71073 Å	0.71073 Å
crystal system	triclinic	triclinic	triclinic	monoclinc
space group	$P\bar{1}$ (No. 2)	$P\bar{1}$ (No. 2)	$P\bar{1}$ (No. 2)	$P2_1/c$ (No. 14)
unit-cell dimensions				
a	7.3882(3) Å	7.2881(3) Å	7.4468(4) Å	6.9953(4) Å
b	8.5223(3) Å	8.9125(2) Å	8.5066(4) Å	15.9420(9) Å
c	9.2712(4) Å	8.9220(4) Å	9.2477(4) Å	9.2299(5) Å
α	71.945(2)°	75.546(2)°	72.321(2)°	
β	88.910(2)°	89.151(2)°	88.512(2)°	100.235(2)°
γ	72.603(2)°	69.516(2)°	72.128(2)°	
volume	527.88(4) $Å^3$	524.02(4) $Å^3$	529.75(4) $Å^3$	1012.45(1) $Å^3$
Z	1	1	1	2
density (calculated)	2.564 g/cm^3	2.564 g/cm^3	2.977 g/cm^3	2.706 g/cm^3
absorption coefficient	18.01 cm^{-1}	18.25 cm^{-1}	63.54 cm^{-1}	19.15 cm^{-1}
F(000)	404	412	456	808
crystal size	0.31 mm × 0.24 mm × 0.02 mm	0.22 mm × 0.18 mm × 0.12 mm	0.23 mm × 0.16 mm × 0.13 mm	0.24 mm × 0.15 mm × 0.06 mm
2*θ* range for data collection	4.64°−80.54°	4.72°−80.54°	4.64°−80.55°	5.12°−80.50°
index ranges	$-13 \le h \le 13$, $-15 \le k \le 15$, $-16 \le l \le 16$	$-13 \le h \le 13$, $-16 \le k \le 16$, $-16 \le l \le 16$	$-12 \le h \le 13$, $-15 \le k \le 15$, $-16 \le l \le 15$	$-7 \le h \le 12$, $-28 \le k \le 28$, $-16 \le l \le 16$
reflections collected	25001	55884	39350	65467
independent reflections	6642 [*R*(int) = 0.0227]	6597 [*R*(int) = 0.0212]	6666 [*R*(int) = 0.0253]	6363 [*R*(int) = 0.0204]
completeness to *θ*	99.8%	100%	99.6%	99.9%
absorption correction	numerical	numerical	numerical	numerical
max and min transmission	0.9615 and 0.6088	0.8500 and 0.7543	0.3252 and 0.5039	0.6523 and 0.8987
data/restraints/parameters	6642/0/185	6597/0/178	6666/0/170	6363/0/169
goodness-of-fit on F^2	1.029	1.108	1.084	1.100
final *R* indices [$I > 2\sigma(I)$]				
R_1	0.0196	0.0156	0.0155	0.0137
wR_2	0.0474	0.0428	0.0393	0.0376
R indices (all data)				
R_1	0.0266	0.0168	0.0171	0.0149
wR_2	0.0497	0.0434	0.0396	0.0381
largest diff. peak and hole	0.78 and −1.33 $e^-/Å^3$	0.68 and −1.24 $e^-/Å^3$	0.57 and −1.10 $e^-/Å^3$	0.59 and −1.18 $e^-/Å^3$
CSD number	425248	426273	425728	425729

DOI: 10.1021/acs.inorgchem.5b00195
Inorg. Chem. 2015, 54, 5681−5690

slightly compressed. In the crystal structures of the compounds $M_2[Pd(S_4O_{13})_2]$ (M = Rb, NO), the $[Pd(S_4O_{13})_2]^{2-}$ anions are arranged into layers parallel to the $a-c$ plane and separated by the M^+ cations (see Figure 3).

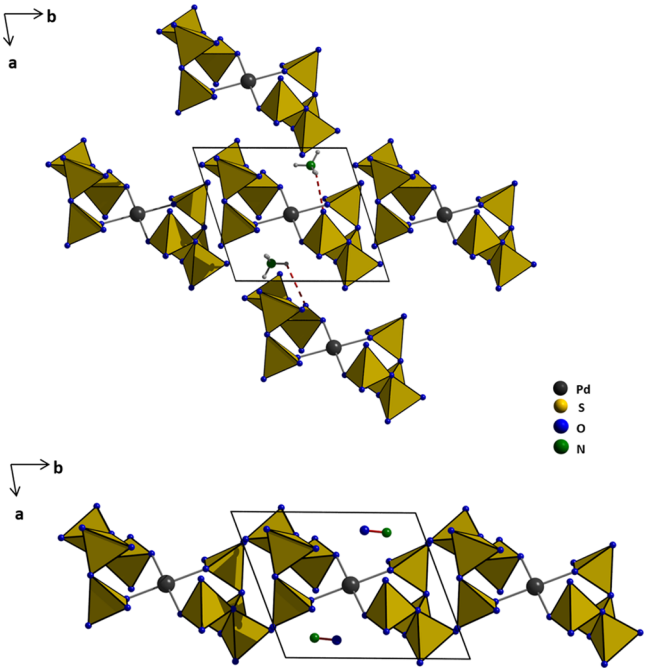

Figure 3. (Top) Crystal structure of $(NH_4)_2[Pd(S_4O_{13})_2]$ in projection onto the (001) plane with hydrogen bridges between N1 and O12 with D−A distance of 2.88.9(2) Å. The structure of the rubidium compound $Rb_2[Pd(S_4O_{13})_2]$ is isotypic. (Bottom) Crystal structure of $(NO)_2[Pd(S_4O_{13})_2]$ in projection onto the (001) plane. The rod-shaped NO^+ cations are orientated along the [010] direction.

3.3. IR Spectra of $M_2[Pd(S_4O_{13})_2]$ (M = NH_4, NO, Rb).

Infrared (IR) spectra were recorded for the tetrasulfatometallates $M_2[Pd(S_4O_{13})_2]$ (M = NH_4, NO, Rb). Theoretically, for a $[Pd(S_4O_{13}]^{2-}$ anion with C_i symmetry, 51 fundamental vibrations could occur in the IR spectrum, all of which belong to the symmetry species A_u. Not all of these possible vibrations are necessarily seen in the spectrum, because they are not resolved or are outside the measuring range (see Figure 4). Theoretical investigations that we have performed previously for $K_2[Pd(S_4O_{13})_2]$ allowed the inspection of fundamental vibrations and their assignment (see Table 4).[26] If possible, the assignment tries to differentiate between vibrations that have main contributions of the inner tetrahedra of the anions ($[S2O_4]$ and $[S3O_4]$) and those having main contribution of the outer tetrahedra ($[S1O_4]$ and $[S2O_4]$). The symmetric and asymmetric deformation modes of all tetrahedra of the anion fall in the same range between 550 cm^{-1} and 700 cm^{-1}. In this region, the bands are comparably sharp and clearly separated. Also, for the stretching vibration modes of the inner S−O−S bridges, sharp bands between 730 cm^{-1} and 800 cm^{-1} are found. The stretching vibration modes of the outer S−O−S bridges are seen as one very broad band at ∼855 cm^{-1}. Also, the bands for the symmetric stretching vibration modes of the terminal S═O bonds are very broad, but with a small shoulder. The strongest bands appear at ∼1020 cm^{-1}, with a weak shoulder uniformly appearing at 1049 cm^{-1}. The bands referring to the symmetric stretching vibration modes of the inner S═O bonds are observed at ∼1205 and 1225 cm^{-1}, respectively. The correlated asymmetric stretching vibration modes of the inner S═O bonds occur between 1380 and 1460 cm^{-1}. For $(NH_4)_2[Pd(S_4O_{13})_2]$, at higher energies, the N−H vibration modes of the NH_4^+ ion can be identified as a very broad band at 3300 cm^{-1} (cf. Figure 4), which is in good accordance with the literature data.[37] Moreover, the N−O stretching vibration is found for the NO^+ ion in $(NO)_2[Pd(S_4O_{13})_2]$ at ∼2312 cm^{-1}. Table 5 summarizes the observed bands and their assignment.

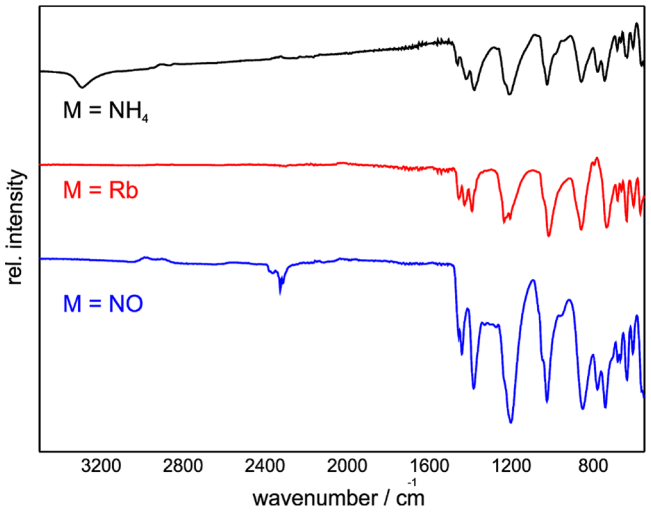

Figure 4. IR data of $M_2[Pd(S_4O_{13})_2]$ (M = NH_4, Rb, NO).

Table 4. Data for the Thermal Decomposition of $M_2[Pd(S_4O_{13})_2]$ (M = Rb, NO, NH_4)

step	$T_{onset}/T_{max}/T_{end}$	expected mass loss (%)	expected product
	$Rb_2[Pd(S_4O_{13})_2]$		
I	140/180/200	16.7	
II	205/270/330	18.6	
III	365/415/460	3.5	
IV/V	510/600 + 845/970	21.3	Pd/Rb_2SO_4
sum		60.1	Pd/Rb_2SO_4
	$(NH_4)_2[Pd(S_4O_{13})_2]$		
I	120/125/130	4.0	
II	140/185/210	28.0	
III/IV	220/225 + 290/335	47.6	$PdSO_4$
V	380/475/550	4.1	PdO
VI	590/655/735	2.5	Pd
sum		86.2	Pd
	$(NO)_2[Pd(S_4O_{13})_2]$		
I	140/195/215	22.2	
II	220/290/360	40.8	
III	500/560/600	10.2	
IV/V	630/720 + 900/990	14.1	Pd
sum		87.3	Pd

3.4. Thermal Decomposition of $M_2[Pd(S_4O_{13})_2]$ (M = NH_4, NO, Rb).

The investigated samples for the TGA/DSC measurements were prepared in a glovebox and transferred to the thermoanalyzer under inert conditions. In the TG curves of all compounds, a slight increase of the mass is observed at low temperature, most significant for the NO compound (see Figure 5). This effect is reproducible, but we currently do not have an explanation. As expected, because of the different counter cations M^+ of the palladates $M_2[Pd(S_4O_{13})_2]$ (M = NH_4, Rb, NO), each of the four palladates show a different

DOI: 10.1021/acs.inorgchem.5b00195
Inorg. Chem. 2015, 54, 5681−5690

Table 5. Experimental IR Energies for $M_2[Pd(S_4O_{13})_2]$ (M = K, NH_4, NO, Rb)[a]

IR Bands (cm^{-1})						
$(NH_4)_2[Pd(S_4O_{13})_2]$	strength[b]	$Rb_2[Pd(S_4O_{13})_2]$	strength[b]	$(NO)_2[Pd(S_4O_{13})_2]$	strength[b]	assignment
565	m	569	m	563	m	
607	m	603	m	606	m	
634	m	638	m	638	m	$\delta_{sym}/\delta_{asym}(SO_3)$
665	w	663	w	664	w	
683	m	682	m	680	m	
744	s	733	s	741	s	ν(S−O−S) *inner*
779	s	796	s	779	s	
860	s	858	s	851	s	ν(S−O−S) *terminal*
1026	s	1018	s	1025	s	
1049	w	1049	w	1049	w	ν_{sym}(S═O) *terminal*
1207	s	1206	s	1202	s	
1224	s	1224	s	1232	s	ν_{sym}(S═O) *inner*
1384	s	1390	s	1384	s	
1418	s	1418	s			ν_{asym}(S═O) *inner*
		1430	m	1440	s	
1461	m	1456	m	1456	s	
				2312	m	ν_{sym}(N−O)
				2325	m	
				2363	b	
3290	b					ν_{sym}(N−H)/ν_{asym}(N−H)

[a]Vibration types labelled with "*inner*" are those with main contributions from the inner terahedra of the tetrasulfate anion, those labeled with "*terminal*" have main contributions from the two outer tetrahedra of the anion. The assignment is based on quantum chemical calculations performed on DFT niveau for the free anion $[Pd(S_4O_{13})_2]^{2-}$.[26] [b]Legend: s = strong, m = medium, w = weak, b = broad.

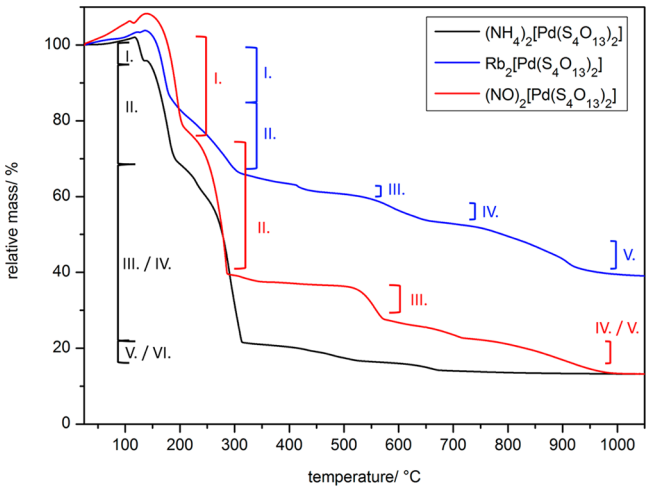

Figure 5. Thermogravimetry (TG) curves of the thermal decomposition of $M_2[Pd(S_4O_{13})_2]$ (M = NO, NH_4, Rb).

decomposition process. To date, we have not been able to identify intermediate products of the decompositions, but the final decomposition residuals were investigated by means of powder X-ray diffraction (XRD). The degradations of the tetrasulfates are stamped by a number of not-well-separated steps. The assignment of these steps has been done on the differentiated TG curves.

For $Rb_2[Pd(S_4O_{13})_2]$, the first decomposition step starts at 140 °C and ends at 200 °C, immediately followed by a subsequent step that arrives at a more or less significant plateau at ~330 °C. The first decomposition step of $Rb_2[Pd(S_4O_{13})_2]$ is accompanied by an experimental mass loss of 16.7%, which might be assigned to the loss of two molecules of SO_3 (calculated mass loss = 16.8%). The additional mass loss of 18.6% during the second step is probably due to the loss of two more SO_3 molecules. A small step with an experimental mass loss of 3.5% is detected between 365 °C and 460 °C. The latter might be attributed to the release of O_2. The fourth and fifth steps for $Rb_2[Pd(S_4O_{13})_2]$ are directly associated, with an experimental mass loss of 21.3%. The onset temperature for the two last steps is determined to be 510 °C, and the end temperature is determined to be 970 °C. Finally, elemental palladium and Rb_2SO_4 are formed, as confirmed by XRD (Figure 6).

The thermal decomposition of $(NO)_2[Pd(S_4O_{13})_2]$ occurs in a five-step process. The onset temperature for the first step is found at 140 °C. This first decomposition step is accompanied by an experimental mass loss of 22.2% at 215 °C. The second step occurs between 220 °C and 360 °C, accompanied by an experimental mass loss of 40.8%. The latter is most likely due to the release of four molecules of SO_3 (calculated mass loss: 38.2%). After a broad plateau, the third step with an onset temperature of 500 °C is is accompanied by a mass loss of 10.2%, which is comparable to a calculated value of 9.5% for the loss of one molecule of SO_3. The third step ends at ~600 °C. In

DOI: 10.1021/acs.inorgchem.5b00195
Inorg. Chem. 2015, 54, 5681−5690

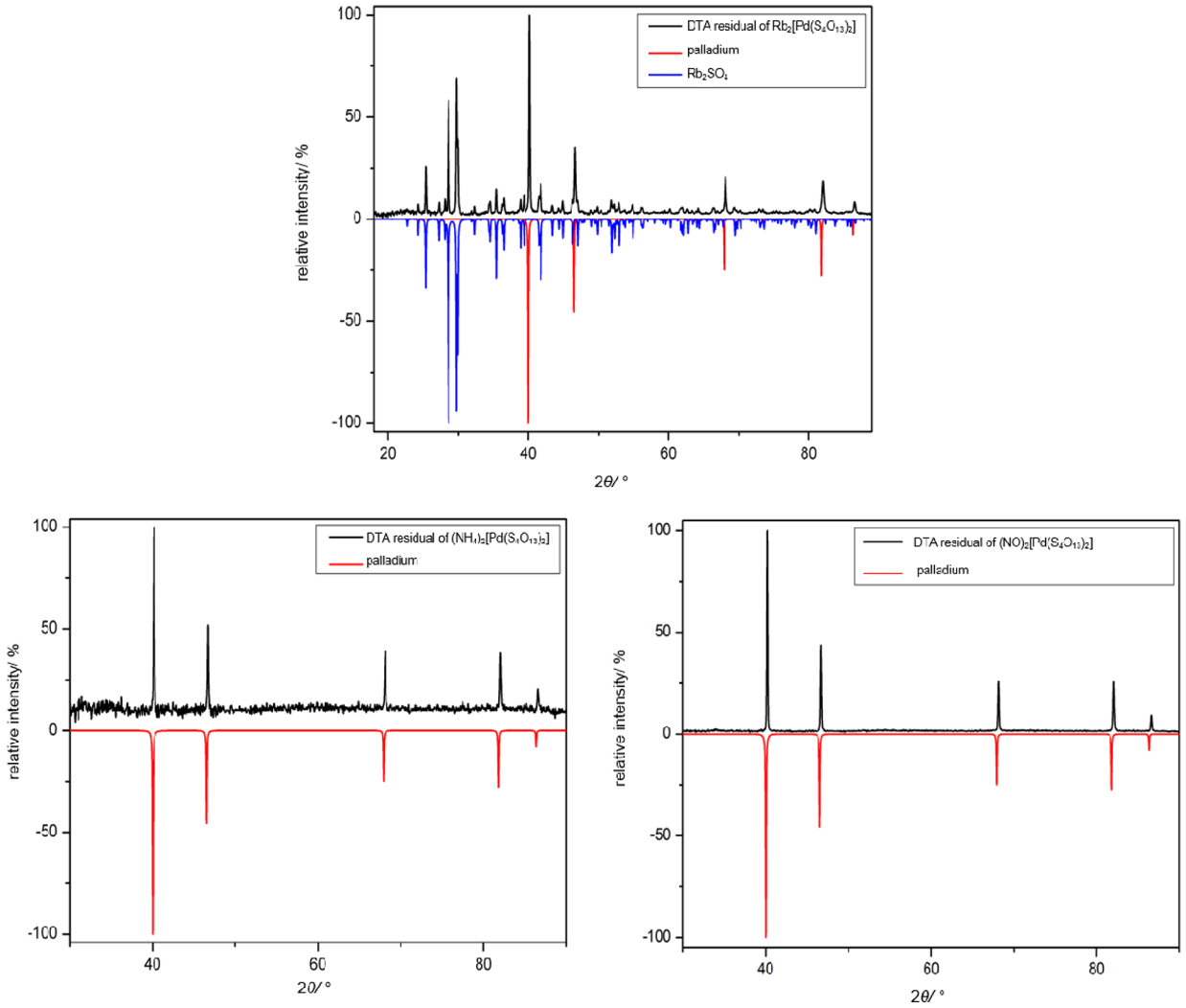

Figure 6. Powder X-ray diffraction (XRD) patterns of the residues of the thermal decomposition of the *bis*-(tetrasulfato)-palladates $M_2[Pd(S_4O_{13})_2]$ (M = Rb, NH_4, NO). The simulated powder patterns are calculated with respect to literature data for Rb_2SO_4 and Pd.[38,39]

addition, a creeping decrease in the TG curve is observed, correlated with a mass loss of 14.1%. According to the powder XRD pattern, the final decomposition product is elemental palladium (see Figure 6).

$(NH_4)_2[Pd(S_4O_{13})_2]$ is the most labile compound within the row of presented tetrasulfates. Not only does the initial decomposition step start at the lowest temperature, but the entire decomposition is also finished at the lowest temperature, resulting in elemental palladium, exclusively. For this tetrasulfate, an almost clearly resolvable five-step process is observed. The first step occurs in the narrow temperature range between 120 °C and 130 °C and shows a small mass loss of 4%, which is consistent with the release of two molecules of NH_3. The next step, with an onset temperature of 140 °C, is accompanied by a mass loss of 28%, which is in good accordance with the expulsion of three molecules of SO_3. The third and fourth step are not separated and are found between 220 °C and 335 °C. The mass loss of 47.6% would match $PdSO_4$ as the intermediate product. Subsequently, the fifth step starts at 380 °C and ends at 550 °C. According to the mass loss of 4.1%, another SO_3 molecule is released. During the last step, between 590 °C and 735 °C, the intermediary formed PdO probably decomposes to elemental palladium, as shown by XRD (recall Figure 6). The last two steps are in good accordance with the previously observed decomposition characteristics of binary palladium sulfates.[26]

3.5. Crystal Structure of $Na_2Pd(S_4O_{13})_2$. In contrast to the palladates $M_2[Pd(S_4O_{13})_2]$ (M = NO, NH_4, Rb), the sodium compound was not obtained quantitatively. A yellowish microcrystalline powder forms as major product that has not been identified yet. At the present stage, we can only report the crystal structure of $Na_2Pd(S_4O_{13})_2$. Although this compound is formally analogous to the palladates discussed above, its structure is completely different. Here, the tetrasulfate anions are not in bidentate-chelating coordination mode but act as bidentate-bridging ligands between two Pd^{2+} ions. In the monoclinic crystal structure (space group $P2_1/c$) group, the Pd atom is located on the special Wyckoff site *2c* bearing inversion symmetry. They are coordinated by four symmetry-equivalent tetrasulfate anions (see Figure 7).

Each of the $S_4O_{13}^{2-}$ anions is connected to an additional Pd^{2+} ion, leading to an infinite layer, according to $^2_\infty[Pd(S_4O_{13})_{4/2}]^{2-}$ (see Figure 8). The coordination sphere around the Pd^{2+} ion is almost ideal square planar, with Pd−O bond lengths of 1.9978(5) Å and 2.0058(5) Å, respectively. Also, the bond angles deviate only slightly from the ideal value and are found at 86.96(2)° and 93.04(2)°. These values fit quite well to the findings for the complex tetrasulfato-palladates.

DOI: 10.1021/acs.inorgchem.5b00195
Inorg. Chem. 2015, 54, 5681−5690

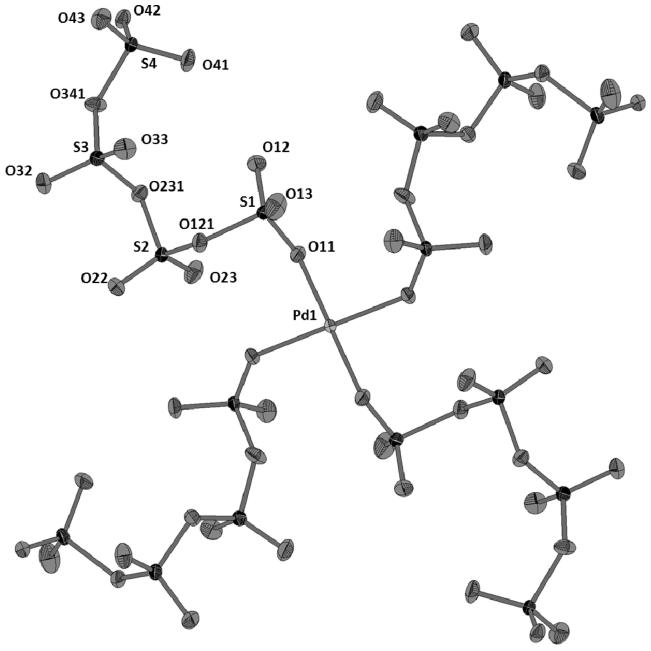

Figure 7. Structure and atom labeling of the $[Pd(S_4O_{13})_4]$ moiety in $Na_2Pd(S_4O_{13})_2$, using the four symmetry-equivalent tetrasulfate anions. The thermal ellipsoids are set at 75% probability.

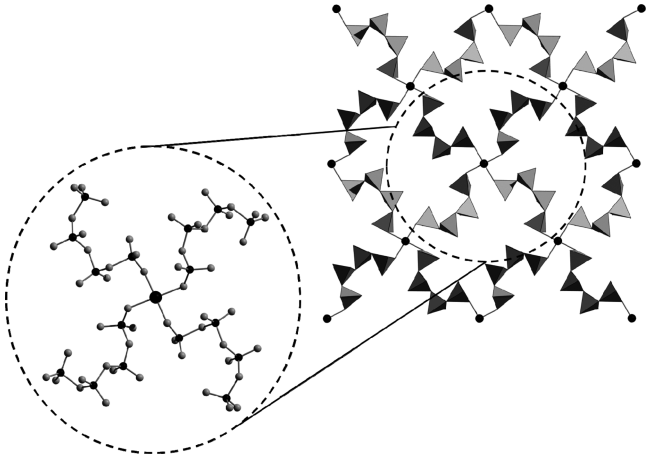

Figure 8. Layers according to $^2_\infty[Pd(S_4O_{13})_{4/2}]^{2-}$ in the crystal structure of $Na_2Pd(S_4O_{13})_2$. The cutoff shows a $[Pd(S_4O_{13})_4]$ unit.

Charge compensation for the $^2_\infty[Pd(S_4O_{13})_{4/2}]^{2-}$ layers is achieved by the Na^+ cations. Each Na^+ cation is coordinated by seven O atoms. The coordination polyhedron could be described as a distorted monocapped octahedron (see Figure 9). The Na−O bond distances range from 2.3610(7) Å to 2.5858(7) Å. The longest distance is found for the capping oxygen atom (O32). The tetrasulfate anions are coordinated to the Na^+ ions in three different modes: bidentate-chelating via two O atoms of two end-standing tetrahedra (Figure 10, **2**), monodentate via an O atom of the terminal tetrahedra (Figure 10, **3**) and monodentate via an O atom of the inner tetrahedral of the tetrasulfate anion (Figure 10, **1**). The Na−O bond lengths are different, with respect to the coordination modes of the tetrasulfate anions. The distances for the chelating anions are comparatively short (2.3610(7) and 2.3967(6) Å). The Na−O distances of the monodentate coordinating O atoms of the terminal $[SO_4]$ moiety show values of 2.3903(6) and

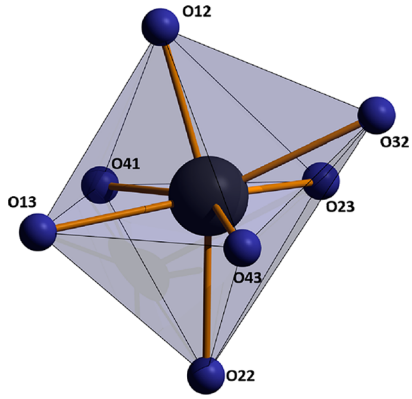

Figure 9. Coordination of Na^+ ions in the structure of $Na_2Pd(S_4O_{13})_2$. The $[NaO_7]$ polyhedron is a capped distorted octahedron. The O atoms originate from tetrasulfate anions, which coordinate either in a bidentate chelating mode or in monodentate fashion by terminal or inner $[SO_4]$ tetrahedra, respectively (cf. Figure 10). Bond lengths, Na−O: Na−O41, 2.3967(7) Å; Na−O43, 2.3903(7) Å; Na−O32, 2.5858(7) Å; Na−O22, 2.4696(7) Å; Na−O23, 2.5705(7) Å; Na−O12, 2.3610(7) Å; and Na−O13, 2.5578(7) Å.

2.5578(7) Å. The longest bond lengths are found between the Na atom and the O atom of the inner tetrahedra of the anion. Those bond lengths have values of 2.4696(79), 2.5705(7), and 2.5858(7) Å, respectively.

Within the tetrasulfate anions, those O atoms that are coordinated to the Pd atoms show bond lengths of 1.4695(5) Å (S1−O11) and 1.4726(5) Å (S4−O42), while the remaining S−O bonds exhibit distances of 1.4104(6)−1.4210(6) Å. According to the values of 1.6039(5) and 1.6397(5) Å, only a slight difference of ∼0.036(1) Å is observed for the S−O bond lengths within the inner S−O−S bridge (recall Table 1). This difference is comparable to the one observed for the free tetrasulfate in $(NO_2)_2(S_4O_{13})$ (Δ = 0.033(1) Å), and slightly larger than those discussed above for the complex palladates $M_2[Pd(S_4O_{13})_2]$ (M = NO, NH_4, Rb). Larger deviations arise for the outer S−O−S bridges. For $Na_2Pd(S_4O_{13})_2$, these bond lengths are found at 1.7015(5) and 1.5613(5) Å for the bridge S1−O121−S2 (Δ = 0.140(1) Å) and at 1.5487(5) and 1.6962(5) Å for the bridge S3−O341−S4 (Δ = 0.144(1) Å). These values are ∼0.09 Å shorter than those discussed for $(NO_2)_2(S_4O_{13})$ and are consistent with the findings for the complex tetrasulfato-palladates $M_2[Pd(S_4O_{13})_2]$ (M = NO, NH_4, Rb) (recall Table 2). This observation means that the bidentate-chelating coordination mode not only leads to a stabilization of the tetrasulfate anions, but also to the bidentate-bridging coordination observed in the sodium compound.

4. CONCLUSION

The compounds presented in this paper are new members of the scarcely investigated family of polysulfates. The key for their preparation is the use of pure SO_3 under high temperature in closed glass ampules. The high SO_3 concentration leads to the formation of the palladium compounds $M_2[Pd(S_4O_{13})_2]$ (M = Rb, NH_4, NO) and $Na_2Pd(S_4O_{13})_2$. The *bis*-(tetrasulfato)-palladates show the Pd atom in chelating coordination of two tetrasulfate anions, while $Na_2Pd(S_4O_{13})_2$ displays tetrasulfate anions in a bidentate-bridging mode. In both cases, the coordination of tetrasulfate anions strongly influences the distances within the anions, when compared to the "naked" $S_4O_{13}^{2-}$ anions in $(NO_2)_2(S_4O_{13})$. Further insight into the

DOI: 10.1021/acs.inorgchem.5b00195
Inorg. Chem. 2015, 54, 5681−5690

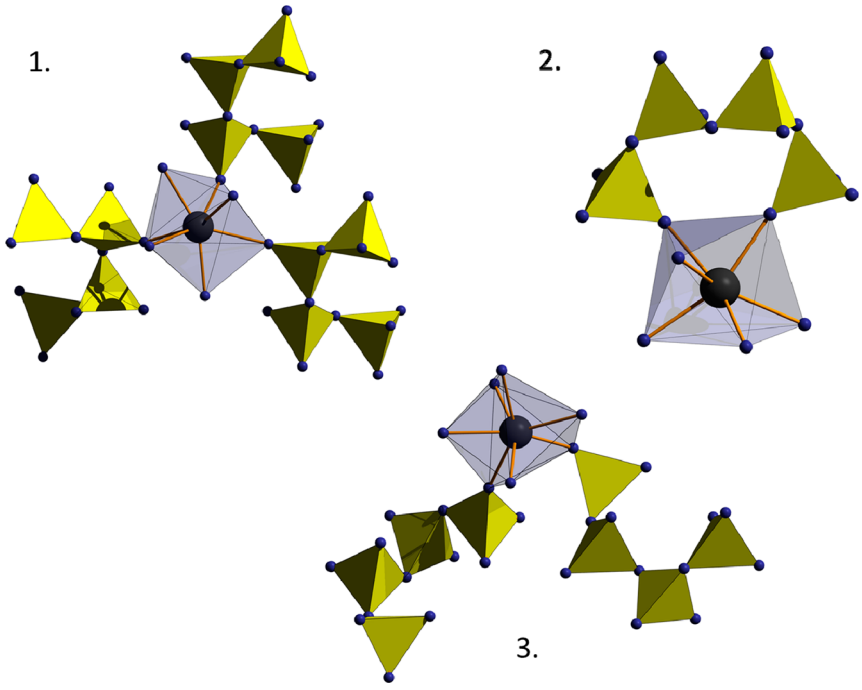

Figure 10. Different coordination modes of tetrasulfate anions bonded to Na^+ cations in the crystal structure of $Na_2Pd(S_4O_{13})_2$: (**1**) monodentate coordination via terminal O atoms of inner $[SO_4]$ tetrahedra; (**2**) monodentate coordination via terminal O atoms of end-standing $[SO_4]$ tetrahedra; and (**3**) bidentate chelating coordination via terminal O atoms of end-standing $[SO_4]$ tetrahedra.

chemistry of polysulfates is gained by infrared spectroscopy and thermoanalysis. With respect to our extremely limited knowedge of polysulfates, we hope that this contribution stimulates further investigations of this very important and fundamental class of compounds.

■ ASSOCIATED CONTENT

Supporting Information

Tables S1−S12 contain the complete crystallographic data and selected bond lengths and angles for the presented compounds. Further details of the crystal structure investigations may be obtained from Fachinformationszentrum Karlsruhe, 76344 Eggenstein-Leopoldshafen, Germany (Fax: (+49)7247-808-666; E-mail: crysdata@FIZ-Karlsruhe.de; URL: http://fiz-karlsruhe.de/request_for_deposited_data.html) by quoting the deposition number given in Table 3. The Supporting Information is available free of charge on the ACS Publications website at DOI: 10.1021/acs.inorgchem.5b00195.

■ AUTHOR INFORMATION

Corresponding Author

*Tel.: +49 (0) 641 99 34100. Fax: +49 (0) 641 99 34109. E-mail: mathias.wickleder@anorg.chemie.uni-giessen.de.

Notes

The authors declare no competing financial interest.

■ ACKNOWLEDGMENTS

Financial support of the *Deutsche Forschungsgemeinschaft*, and the *Stiftung der Metallindustrie im Nordwesten* is gratefully acknowledged. We thank Dr. Marc Schmidtmann and Dipl. Chem. Wolfgang Saak for the collection of the X-ray data.

■ REFERENCES

(1) Hoenle, W. *Z. Kristallogr.* **1991**, *196*, 279−288.
(2) Steeman, J. W. M.; MacGillavry, C. H. *Acta Crystallogr.* **1954**, *7*, 402−404.
(3) Lynton, H.; Truter, M. R. *J. Chem. Soc.* **1960**, 5112−5118.
(4) Brown, I. D.; Crump, D. B.; Gillespie, R. J. *Inorg. Chem.* **1971**, *10*, 2319−2323.
(5) Douglade, J.; Mercier, R. *Acta Crystallogr., Sect. B: Struct. Crystallogr. Cryst. Chem.* **1979**, *B35*, 1062−1067.
(6) Einstein, F. W. B.; Willis, A. C. *Acta Crystallogr., Sect. B: Struct. Crystallogr. Cryst. Chem.* **1981**, *B37*, 218−220.
(7) Simonov, M. A.; Shkovrov, S. V.; Troyanov, S. I. *Kristallografiya* **1988**, *33*, 502−503.
(8) Jansen, M.; Müller, R. *Z. Anorg. Allg. Chem.* **1997**, *623*, 1055−1060.
(9) Wickleder, M. S. *Z. Anorg. Allg. Chem.* **2000**, *626*, 621−622.
(10) Stahl, K.; Balic Zunic, T.; Da Silva, F.; Eriksen, K. M.; Berg, R. W.; Fehrmann, R. *J. Solid State Chem.* **2005**, *178*, 1697−1704.
(11) Stahl, K.; Berg, R. W.; Eriksen, K. M.; Fehrmann, R. *Acta Crystallogr., Sect. B: Struct. Sci.* **2009**, *B65*, 551−557.
(12) Betke, U.; Dononelli, W.; Klüner, T.; Wickleder, M. S. *Angew. Chem.* **2011**, *123*, 12569−12571; *Angew. Chem., Int. Ed.* **2011**, *50*, 12361−12363.
(13) Logemann, C.; Klüner, T.; Wickleder, M. S. *Chem.—Eur. J.* **2011**, *17*, 758−760.
(14) Logemann, C.; Wickleder, M. S. *Inorg. Chem.* **2011**, *50*, 11111−11116.
(15) Betke, U.; Wickleder, M. S. *Eur. J. Inorg. Chem.* **2011**, *28*, 4400−4413.
(16) Logemann, C.; Rieß, K.; Wickleder, M. S. *Chem.—Asian J.* **2012**, *7*, 2912−2920.
(17) Logemann, C.; Witt, J.; Gunzelmann, D.; Senker, J.; Wickleder, M. S. *Z. Anorg. Allg. Chem.* **2012**, *638*, 2053−2061.
(18) Betke, U.; Wickleder, M. S. *Eur. J. Inorg. Chem.* **2012**, *2*, 306−317.
(19) Bruns, J.; Eul, M.; Pöttgen, R.; Wickleder, M. S. *Angew. Chem.* **2012**, *124*, 2247−2250; *Angew. Chem., Int. Ed.* **2012**, *51*, 2204−2207.
(20) Eriks, K.; MacGillavry, C. H. *Acta Crystallogr., Sect. B: Struct. Crystallogr. Cryst. Chem.* **1954**, *B7*, 430−434.
(21) Cruickshank, D. W. J. *Acta Crystallogr.* **1964**, *17*, 684.

DOI: 10.1021/acs.inorgchem.5b00195
Inorg. Chem. 2015, 54, 5681−5690

(22) Logemann, C.; Klüner, T.; Wickleder, M. S. *Z. Anorg. Allg. Chem.* **2012**, *638*, 758−762.
(23) Bruns, J.; Klüner, T.; Wickleder, M. S. *Chem.—Asian J.* **2014**, *6*, 1594−1600.
(24) de Vries, R.; Mijlhoff, F. C. *Acta Crystallogr., Sect. B: Struct. Crystallogr. Cryst. Chem.* **1969**, *B25*, 1696.
(25) Logemann, C.; Klüner, T.; Wickleder, M. S. *Angew. Chem.* **2012**, *124*, 5082−5085; *Angew. Chem., Int. Ed.* **2012**, *51*, 4997−5000.
(26) Bruns, J.; Klüner, T.; Wickleder, M. S. *Angew. Chem.* **2013**, *125*, 2650−2652; *Angew. Chem., Int. Ed.* **2013**, *52*, 2590−2592.
(27) Brauer, G. *Handbuch der Präparativen Anorganischen Chemie*; F. Enke, Stuttgart, Germany, 1975, 1729.
(28) Wickleder, M. S.; Gerlach, F.; Gagelmann, S.; Bruns, J.; Fenske, M.; Al-Shamery, K. *Angew. Chem.* **2012**, *124*, 2242−2246; *Angew. Chem., Int. Ed.* **2012**, *51*, 2199−2203.
(29) Sheldrick, G. M. *Acta Crystallogr., Sect. A: Found. Crystallogr.* **2008**, *A64*, 112−122.
(30) *X-RED 1.22*; Stoe & Cie: Darmstadt, Germany, 2001.
(31) *X-SHAPE 1.06*; Stoe & Cie: Darmstadt, Germany, 1999.
(32) *SADABS*; Bruker: Madison, WI, USA, 2001.
(33) *Star^{e} V 9.3*; Mettler-Toledo GmbH: Schwerzenbach, Switzerland, 2009.
(34) *WinXPOW 2007*; Stoe & Cie: Darmstadt, Germany, 2006.
(35) *OPUS 6.5*; Bruker Optik GmbH: Germany, 2009.
(36) Hoppe, R. *Z. Kristallogr.* **1979**, *150*, 23−52.
(37) Hesse, M.; Meier, H.; Zeeh, B. *Spektroskopische Methoden in der Organischen Chemie*; Thieme Verlag: Stuttgart, Germany, 2002.
(38) Haglund, J.; Fernandez Guillerment, F.; Grimvall, G.; Korling, M. *Phys. Rev.* **1993**, *B48*, 11685−11691.
(39) Nord, A. G. *Acta Crystallogr., Sect. B: Struct. Crystallogr. Cryst. Chem.* **1974**, *B30*, 1640−1641.

DOI: 10.1021/acs.inorgchem.5b00195
Inorg. Chem. 2015, 54, 5681−5690